

Butterfly velocity and bulk causal structure

Xiao-Liang Qi¹, Zhao Yang¹

¹*Department of Physics, Stanford University, Stanford, CA 94305, USA*

Abstract

The butterfly velocity was recently proposed as a characteristic velocity of chaos propagation in a local system. Compared to the Lieb-Robinson velocity that bounds the propagation speed of all perturbations, the butterfly velocity, studied in thermal ensembles, is an "effective" Lieb-Robinson velocity for a subspace of the Hilbert space defined by the microcanonical ensemble. In this paper, we generalize the concept of butterfly velocity beyond the thermal case to a large class of other subspaces. Based on holographic duality, we consider the code subspace of low energy excitations on a classical background geometry. Using local reconstruction of bulk operators, we prove a general relation between the boundary butterfly velocities (of different operators) and the bulk causal structure. Our result has implications in both directions of the bulk-boundary correspondence. Starting from a boundary theory with a given Lieb-Robinson velocity, our result determines an upper bound of the bulk light cone starting from a given point. Starting from a bulk space-time geometry, the butterfly velocity can be explicitly calculated for all operators that are the local reconstructions of bulk local operators. If the bulk geometry satisfies Einstein equation and the null energy condition, for rotation symmetric geometries we prove that infrared operators always have a slower butterfly velocity than the ultraviolet one. For asymptotic AdS geometries, this also implies that the butterfly velocities of all operators are upper bounded by the speed of light. We further prove that the butterfly velocity is equal to the speed of light if the causal wedge of the boundary region coincides with its entanglement wedge. Finally, we discuss the implication of our result to geometries that are not asymptotically AdS, and in particular, obtain constraints that must be satisfied by a dual theory of flat space gravity.

Contents

1	Introduction	1
2	Definition of the butterfly velocity	4
3	Boundary time evolution and bulk causality	5
3.1	An overview of the local reconstruction property	6
3.2	Bound on bulk light cone	7
4	Bulk speed of light determines boundary butterfly velocities	10
5	General properties of butterfly velocity	14
5.1	Monotonicity	14
5.2	When is the butterfly velocity equal to c ?	16
6	Examples	18
6.1	Pure AdS and BTZ black hole	18
6.2	Higher dimensional AdS Schwarzschild black hole	18
7	Flat space	21
8	Conclusion and discussion	23
A	Precise definition of butterfly velocity	25
B	Monotonicity of butterfly velocity of operators in the same region	26
C	Proof of the saturation of butterfly velocity when the causal wedge coincides with the entanglement wedge	29
D	Flat space holography	31

1 Introduction

The butterfly velocity [1,2] is generally a *state dependent* measure of the quantum many-body dynamics that quantifies the propagation velocity of the causal influence for a local perturbation *when the influence is probed in a subspace of many-body states*. For a relativistic system, the velocity of causal influence is the speed of light if we study a generic perturbation acting on arbitrary quantum states. However, the butterfly velocity at finite temperature is generically slower than the speed of light because we are probing the causal influence only in states with a fixed energy density. The butterfly velocity can

be measured by the effective size of commutator between local operators. In large N theories with a semi-classical holographic dual, the commutator is believed to behave as $\langle [W(x, t), V(0, 0)]^2 \rangle_\beta = \frac{C}{N^2} e^{\lambda_L(t-x/v_B)} + O(N^{-4})$, where W, V are the generic operators, C is a constant, λ_L is the Lyapunov exponent, and v_B is the butterfly velocity. $\langle \rangle_\beta$ represents the thermal average at temperature $1/\beta$. Moreover, according to the anti-de Sitter/conformal field theory (AdS/CFT) correspondence [3–5], the large N gauge theory at finite temperature is dual to the AdS black hole geometry, and applying boundary operators onto the thermal ensemble corresponds to shooting shock waves into the black hole in the bulk [1, 2]. Thus the butterfly velocity can be calculated holographically in the bulk by evaluating the back-reaction of the shock wave geometry [1, 2, 6]. Another independent calculation [7] of the butterfly velocity was accomplished by studying the expansion rate of the extremal surface near the black hole horizon. This result is consistent with previous shockwave calculations. However, all the discussions on butterfly velocities so far are about the thermal ensembles. Also, as will be seen from the results of the present paper, the butterfly velocities calculated in these previous works only correspond to those bulk operators close to the horizon.

Motivated by these works, our paper aims to generalize the concept of butterfly velocity beyond the thermal ensemble to more generic subspaces of states. We observe that in the same code-subspace different operators generically have different velocities, and we establish a concrete relation between the boundary butterfly velocity and the bulk causal structure in holographic systems. The connection between these two ends is the quantum error correction conditions, which have been observed both within the AdS/CFT correspondence [8–11] and in the tensor network models [12–16]. A natural generalization of the thermal ensemble is the code subspace, *i.e.*, the subspace of small fluctuations around a classical geometry. The code subspace for an AdS black hole includes states with a fixed energy density from a (microcanonical) thermal ensemble of the boundary. Holographically, these states are dual to the same classical black-hole geometry. However, they are different black-hole micro-states or have different states in the effective field theory living on top of the black hole geometry. We demonstrate that the concept of the butterfly velocity can be generalized to arbitrary code subspaces, and it is defined as the propagation velocity of certain operators measured by the states in the code subspace. For large N theories with a semi-classical bulk dual, using the entanglement wedge reconstruction, we prove that the bulk causal structure determines the butterfly velocities of operators on the boundary and vice versa. Our generalization of the butterfly velocity not only reproduces all the results in the thermal ensembles, but also allows us to predict the boundary but-

terfly velocities in more general boundary states with classical bulk dual geometries, such as time-dependent geometries. Our generalized butterfly velocity is operator-specific. For local operators in the bulk that are mapped to boundary operators in the same disk-shape region, we prove that butterfly velocity of the operator deeper in the bulk is slower for any geometry that satisfied Einstein's equation (EE) and the null energy condition (NEC). In addition, using tensor network construction, one can even construct spatial geometries that are not asymptotically AdS while still preserving error correction properties of the bulk-boundary correspondence. Our discussion also applies for such geometries and impose constraints on the possible dual theories. In particular, we study the example of a flat geometry, and show that the boundary theory has to have a divergent butterfly velocity, which therefore has to be a nonlocal theory.

The remainder of the paper is organized as follows. In Sec.2, we give the precise definition of the butterfly velocity, for a given operator and a given code subspace. Then in Sec.3, we analyze the indication of this definition to the bulk theory. We show that in a holographic mapping with error correction properties, such as the random tensor network models [14,15], the Lieb-Robinson velocity of the boundary, which is the upper bound of the butterfly velocities, determines an upper bound of the speed of light in the bulk. Running this argument on different regions of the boundary, we obtain a bulk region that encloses the casual future of a bulk point. The physical interpretation of this result is that the quantum error correction properties and local boundary dynamics imply the local bulk dynamics in the code subspace. Specifically, in the random tensor network models, this result means that the holographic mapping defined by random tensor networks always maps local boundary dynamics to local bulk dynamics in the code subspace. In sections 4-7, we focus on the bulk-to-boundary direction and derive the properties of boundary butterfly velocities from a known bulk space-time geometry. In Sec.4, we show that in the holographic theory the light cone at the bulk point x determines the butterfly velocity of the boundary operators that are local reconstruction of a local bulk operator at x . In Sec.5.1, we assume the bulk geometry to satisfy the Einstein equation (EE) and the null energy condition (NEC) and conclude that, roughly speaking, the butterfly velocities of the boundary operators decrease monotonically from the UV to IR. The precise statement can be found in Sec.5.1. This conclusion also implies that if the bulk geometry is asymptotically AdS, the butterfly velocities of boundary operators are upper bounded by the speed of the light. Furthermore, in Sec.5.2, we prove that, if the bulk geometry is asymptotic AdS that satisfies EE and NEC, and if the causal wedge of the boundary region A coincides with its entanglement wedge, then the butterfly velocities of

the boundary operators that are supported on the whole boundary region A saturate the speed of the light. In Sec.6, we show some explicit calculations of the butterfly velocity for simple bulk geometries, such as $d + 1$ -dimensional pure AdS space, the 3d Banados, Teitelboim and Zanelli (BTZ) black hole [17], and $d + 1$ ($d > 2$) AdS Schwarzschild black holes. In Sec.7, we go beyond AdS/CFT correspondence and study the consequence of our results for a flat bulk geometry. Our results lead to necessary conditions for a boundary theory to have a flat bulk dual. Finally we conclude in Sec.8.

2 Definition of the butterfly velocity

Previous discussions on the butterfly velocities are based on the assumption that the expectation value of commutator square of two operators in a thermal ensemble has the following behavior $\langle [W(x, t), V(0, 0)]^2 \rangle_\beta \propto e^{\lambda_L(t - x/v_B)}$, in which case v_B is called the butterfly velocity. If we use a microcanonical ensemble instead of the canonical one, the quantity $\langle [W(x, t), V(0, 0)]^2 \rangle_\beta$ is the two norm of the commutator in the subspace of states in the microcanonical ensemble. In the following, we will generalize the definition of butterfly velocities from thermal ensemble to more general subspaces. The generalized butterfly velocity describes the maximal information propagation velocity in a given subspace of the Hilbert space.

We set the notations as follows. For a system with locality, such as a system defined in a Riemann manifold, or a discrete system defined on a graph, we define two regions A and B , and denote $d(B, A)$ to be the distance between them, defined as the minimum of distance between two points $x \in A$, $y \in B$. We denote $\{R | d(R, A) = D\}$ as all the regions whose distance to A is D . Besides, if an operator O_A commutes with all operators (in Heisenberg picture) in the region B at time t sandwiched by two states $|\psi_i\rangle$, $|\psi_j\rangle$, then we abbreviate this relation as

$$\langle \psi_i | [O_A, B(t)] | \psi_j \rangle = 0 \quad (1)$$

Now we consider a system with holographic duality and start from the boundary system. Given a boundary code subspace \mathcal{H}_c (which at this moment can be any subspace of the Hilbert space \mathcal{H}), and a generic boundary operator O_A with support on region A , we define the butterfly velocity $v(O_A; \mathcal{H}_c)$ as the minimal velocity such that in the $\Delta t \rightarrow 0$ limit, $\forall B \in \{R | d(R, A) = v(O_A; \mathcal{H}_c)\Delta t\}$, $\forall |\psi_i\rangle, |\psi_j\rangle \in \mathcal{H}_c$,

$$\langle \psi_i | [O_A, B(\Delta t)] | \psi_j \rangle = 0 \quad (2)$$

The precise meaning of $\Delta t \rightarrow 0$ limit in the ϵ, δ language is elaborated in Appendix.A. In fact, it is more realistic to require the commutator to be small, controlled by a small parameter in the system, rather than exactly vanish. For large N theories with a semiclassical dual, the small parameter is $\frac{1}{N}$, and the transition from zero and nonzero commutator at the “butterfly cone” is sharp in the large N limit. All our discussion below applies to such large N limit.

Intuitively, the definition above means that at a small time Δt , operator O_A evolve to a Heisenberg operator $O_A(\Delta t)$ that is “effectively” supported in a region that is a slight expansion of A by the distance $v(O_A; \mathcal{H}_c)\Delta t$. In other words, O_A still commutes with all operators in the complement of this small expansion of A after the Heisenberg evolution, *if the commutator operator is only measured in the code subspace \mathcal{H}_c* . First of all, we know that as long as $v(O_A; \mathcal{H}_c)$ is big enough, it is obvious that Eq.2 is satisfied. For example, if $v(O_A; \mathcal{H}_c) > c$, then obviously all the operators in the boundary region $B \in \{R | d(R, A) = v(O_A; \mathcal{H}_c)\Delta t\}$ at time Δt commutes with O_A . Thus we minimize $v(O_A; \mathcal{H}_c)$ to find the butterfly velocity.

The definition above applies to any subspace \mathcal{H}_c of the boundary Hilbert space, although what we will be interested in are the subspaces in which the bulk-to-boundary isometry with error correction properties is defined. [8] It should be clarified that both operators that appear in the commutator (O_A and generic operators $O_B(\Delta t)$ in $B(\Delta t)$) act on the whole Hilbert space, although the butterfly velocity only measures the norm of the commutator in the code subspace \mathcal{H}_c . Actually, for the code subspace we are interested in, all operators that only act in the code subspace are global on the boundary, so that any local operator like O_A is necessarily coupling the code subspace with its complement in the full Hilbert space.

3 Boundary time evolution and bulk causality

The relation between the butterfly velocity on the boundary and the bulk causal structure is bidirectional. In this section, we look at the direction from the boundary to the bulk. We will show that the boundary butterfly velocities and local reconstruction properties together give bounds on the causal structure of the bulk dual theory.

3.1 An overview of the local reconstruction property

Our results apply generally to systems with a holographic operator correspondence between bulk and boundary with local reconstruction properties, which include the standard AdS/CFT systems [8–11] and holographic mappings defined by tensor networks [12–14]. For concreteness, we briefly overview the local reconstruction property and code subspace in the random tensor networks studied in Ref. [14]. The readers who are already familiar with local reconstruction can skip this subsection.

A random tensor network with dangling legs in both bulk and boundary, as is illustrated in Fig. 1, defines a linear map between the bulk and boundary Hilbert spaces. Each tensor can be considered as an operator V_x with matrix element $V_{x;\alpha\beta\gamma}^a$, which maps the bulk state a to in-plane states $\alpha\beta\gamma$. Then the contraction of internal lines is equivalent to projecting the state of the two ends of a link into a maximally entangled state $|xy\rangle$. The holographic mapping from bulk to boundary is defined as an operator

$$M = \prod_{\langle xy \rangle} \langle xy | \prod_x V_x \quad (3)$$

We denote the dimension of bulk vertex index a as D_b and that of the boundary and the internal indices as D . If there are V vertices in the bulk and V_B vertices on the boundary, the bulk Hilbert space dimension is D_b^V and that of the boundary is D^{V_B} . Ref. [14] proves that the mapping M is an isometry in the limit $D \rightarrow \infty$ with D_b finite. In this case the bulk Hilbert space is mapped by M to a subspace of the boundary Hilbert space, which is the code subspace \mathcal{H}_c we are interested in here. In addition to the isometry property, Ref. [14] also proves the following local reconstruction property, similar to that in AdS/CFT. Each boundary region A is associated with a minimal area surface γ_A bounding it, and the region between A and γ_A is called the entanglement wedge of A , denoted by E_A .¹ For an operator in the bulk ϕ with support in a bulk region R , if we choose a boundary region A such that $R \subset E_A$, then there exists a boundary operator O_A supported in region A , such that $O_A|\psi\rangle = M\phi M^\dagger|\psi\rangle$ for any state $|\psi\rangle \in \mathcal{H}_c$. Since a bulk region R can be enclosed by entanglement wedges of different boundary regions, there are multiple boundary operators which reconstruct the same bulk operator in the code subspace. These different boundary operators are clearly different operators in the entire boundary Hilbert space, but their matrix elements are identical when acting on the code subspace states.

¹More precisely, E_A here corresponds to a spatial slice in the space-time entanglement wedge in the AdS/CFT case.

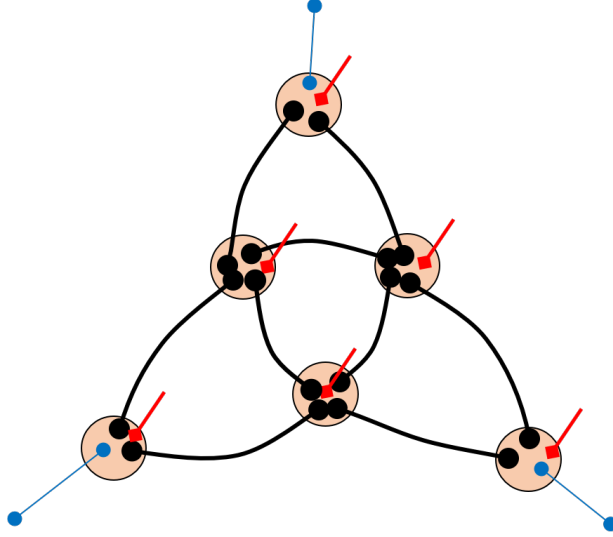


Figure 1: Illustration of a random tensor network, which defines a linear map between the bulk (red legs) and the boundary (blue legs).

The definition of code subspace and local reconstruction properties in AdS/CFT is the same as the tensor network case reviewed above, with the graph geometry replaced by a Riemann geometry. The bulk operators in the code subspace are quantum field theory operators with energy of order 1 which do not change the background geometry to the leading order of Newton constant G_N .

3.2 Bound on bulk light cone

In general, it is complicated to decide the butterfly velocity for all operators. However, the butterfly velocity is upper bounded by the speed of light c for a Lorentz invariant theory, or the Lieb-Robinson velocity v_{LR} for a lattice system [18–20]. Using this upper bound which we denote as v_{LR} , we can determine the upper bound of the light-cone size in the bulk.

For a bulk point x , as is shown in Fig. 2 (a), we consider a boundary region A such that the entanglement wedge E_A barely includes x . More precisely, $x \in E_A$ and x is a distance ϵ away from the minimal surface γ_A , with $\epsilon \rightarrow 0^+$. According to local reconstruction, for any bulk local operator ϕ_x acting at site x , there is a corresponding boundary operator O_A supported on A which is the reconstruction of ϕ_x . If the boundary butterfly velocity for arbitrary operator is upper bounded by v_{LR} , after time Δt the operator O_A will evolve to some operator that is supported in a slightly bigger region $A_{v_{LR}\Delta t}$, which is an expansion

of A defined by the following:

$$A_{v_{LR}\Delta t} \equiv \{x \in \text{boundary} \mid \exists y \in A, \text{ s.t. } d(x, y) \leq v_{LR}\Delta t\} \quad (4)$$

In other words, $A_{v_{LR}\Delta t}$ is the union of all balls of size $v_{LR}\Delta t$ (in the boundary) with center position in A . Since $O_A(\Delta t)$ is supported in $A_{v_{LR}\Delta t}$, it commutes with all boundary operators in its complement, which we denote as $B = \overline{A_{v_{LR}\Delta t}}$. As a consequence, it also commutes with all bulk operators in the code subspace that are supported in the entanglement wedge of the complement region E_B . In other words, the bulk operator ϕ_x is evolved by the boundary time evolution to an operator $\phi_x(\Delta t)$ which is supported in the entanglement wedge of $A_{v_{LR}\Delta t}$, denoted as $E_{A_{v_{LR}\Delta t}} = \overline{E_B}$. In short we can denote

$$\phi_x(\Delta t) \in E_{A_{v_{LR}\Delta t}} \quad (5)$$

For a fixed point x , one can define an infinite family of minimal surfaces passing x , which corresponds to an infinite family of boundary regions. The argument above applies to each such region, so that $\phi_x(\Delta t)$ actually is supported in the intersection of the entanglement wedges $E_{A_{v_{LR}\Delta t}}$ for all these region choices (Fig. 2 (b)):

$$\phi_x(\Delta t) \in D(x, \Delta t) \equiv \bigcap_{A: x \in \gamma_A} E_{A_{v_{LR}\Delta t}} \quad (6)$$

This result shows that arbitrary local perturbation at x , as long as it is in the code subspace, can only spread in the intersection region $D(x, \Delta t)$ after time Δt . If the location of minimal surface γ_A is a continuous function of the boundary region A , the intersection $D(x, \Delta t)$ is a disk which shrinks to point x in the $\Delta t \rightarrow 0$ limit. In a spacetime picture, the union of $D(x, \Delta t)$ for all Δt is a spacetime region that the bulk light cone starting from point x must reside in. Taking $\Delta t \rightarrow 0$, we obtain upper bound of bulk speed of light if $D(x, \Delta t)$ shrinks to zero.

In summary, we have shown that the local reconstruction property and boundary locality (finite v_{LR}) put constraints on locality of bulk dynamics. We would like to make a few further comments here.

Firstly, our starting point in this section is a holographic mapping with error correction properties, defined by a spatial geometry. We are always assuming the minimal surfaces passing x resides in a particular spatial slice, so that RT formula applies. Our result shows that if the spatial geometry is time translational invariant, the local reconstruction constrains the causal structure in the bulk. Our discussion can be generalized to a time-dependent spatial geometry (which means we are using different holographic code

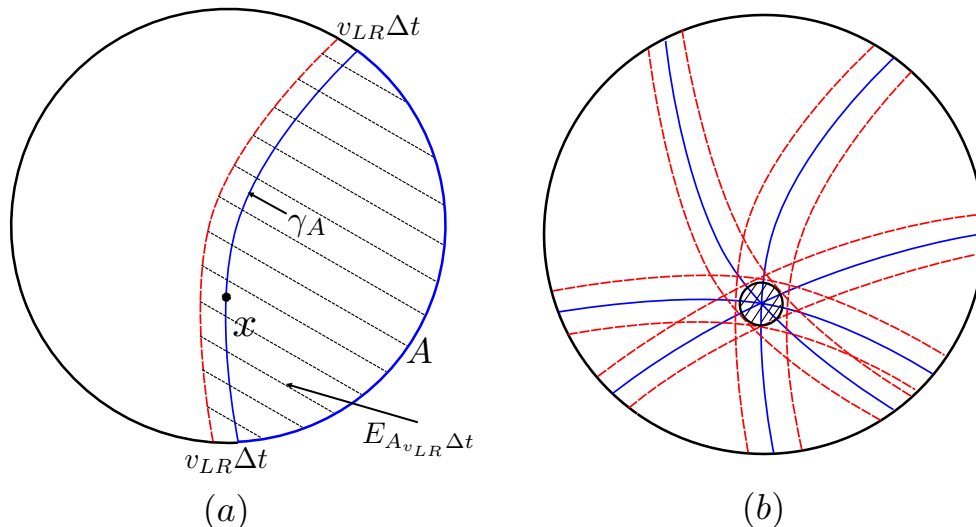


Figure 2: Illustration of the bound on causal future of a point x in the bulk. (a) A bulk local operator ϕ_x at a point x on the minimal surface γ_A can be reconstructed to a boundary region A . The slightly bigger region $A_{v_{LR}\Delta t}$ is defined as the expansion of A by size $v_{LR}\Delta t$ (see text). The shaded region is the entanglement wedge of the bigger region $E_{A_{v_{LR}\Delta t}}$. $\phi_x(\Delta t)$ commutes with all bulk (Schoerdinger) operators outside the shaded region. (b) By repeating the construction in (a) for different boundary regions that reconstruct ϕ_x , we obtain a domain around x by the intersection of entanglement wedges $E_{A_{v_{LR}\Delta t}}$ for different A , which is the upper bound of causal future of x since $\phi_x(\Delta t)$ commutes with all bulk operators outside this region.

at different time), but that requires the assumption that the extremal surfaces bounding boundary regions at a given time all reside in a single bulk slice, which is generically not true.

Secondly, for geometries with minimal surface experiencing topology change, our construction may not apply. For example, in the black hole geometries generically there is a region near the horizon called “entanglement shadow” [21, 22], where no minimal surface bounding any boundary region can reach. An operator ϕ_x in the entanglement shadow can only be reconstructed to a boundary region whose entanglement wedge includes the entire black hole and the entanglement shadow region. In this case, our construction results in a $D(x, \Delta t)$ that remains finite at small Δt . $D(x, \Delta t \rightarrow 0)$ will be the entire entanglement shadow. Therefore the locality of physics in the entanglement shadow region cannot be understood from local reconstruction. It is an interesting open question what is the reason, from boundary dynamics, of bulk locality in the entanglement shadow.

In a geometry with entanglement shadow, for points outside the entanglement shadow

our construction applies. However, the presence of the entanglement shadow still has a nontrivial effect on the upper bound we obtain. Consider the set of all geodesic surfaces which are minimal surfaces of boundary regions, and include point x . As is shown in Fig. 3 (a), in a geometry with entanglement shadow, the normal direction of such surfaces are restricted to certain directions, while in a geometry without entanglement shadow the geodesic surfaces can pass point x along any direction. As a consequence, the domain we obtained by our procedure (expanding minimal surfaces outwards and taking the overlap of their entanglement wedges) leads to a small wedge with corners, rather than a disk. As an example, in Fig. 3 we show the situation in a BTZ black hole. Starting from a geodesic that bounds half of the boundary (red solid curve), we move the geodesic while fix a point x on it. Such motion ends at the red dashed line which bounds a different region that also has half the boundary size. The geodesic cannot move further beyond this point while still includes x . The intersection of small expansion of these geodesics give a diamond shape region (3 (b)) which means the bound on speed of light along the corner directions are loose. When point x moves closer and closer to the entanglement shadow, the bound along the corner direction (which is the direction parallel to the black hole horizon) becomes worse and worse. When x enters the entanglement shadow, local reconstruction does not give bound to bulk locality any more.

4 Bulk speed of light determines boundary butterfly velocities

In this section, we discuss the other direction of the correspondence. Given a holographic theory with a known bulk space-time geometry, we would like to determine the butterfly velocity of a large family of boundary operators. The reasoning is closely related to the discussion in the previous section. For a boundary operator O_A supported in region A which is a local reconstruction of bulk local operator ϕ_x , we obtain an upper bound of the speed of light at point x from the fact that O_A cannot expand in space (of the boundary) faster than v_{LR} . Conversely, if we assume the exact speed of light at x , rather than its upper bound, ‘is already known, this generically imply a slower expansion speed of the dual operator O_A , which is its butterfly velocity.

In contrast to the previous section, since we now assume the bulk space-time geometry is given, we can work with a generally time-dependent geometry in which the entanglement entropy of a boundary region A is given by the extremal surface area defined by the Hubeny-Rangamani-Takayanagi (HRT) formula [23, 24]. The entanglement wedge of a

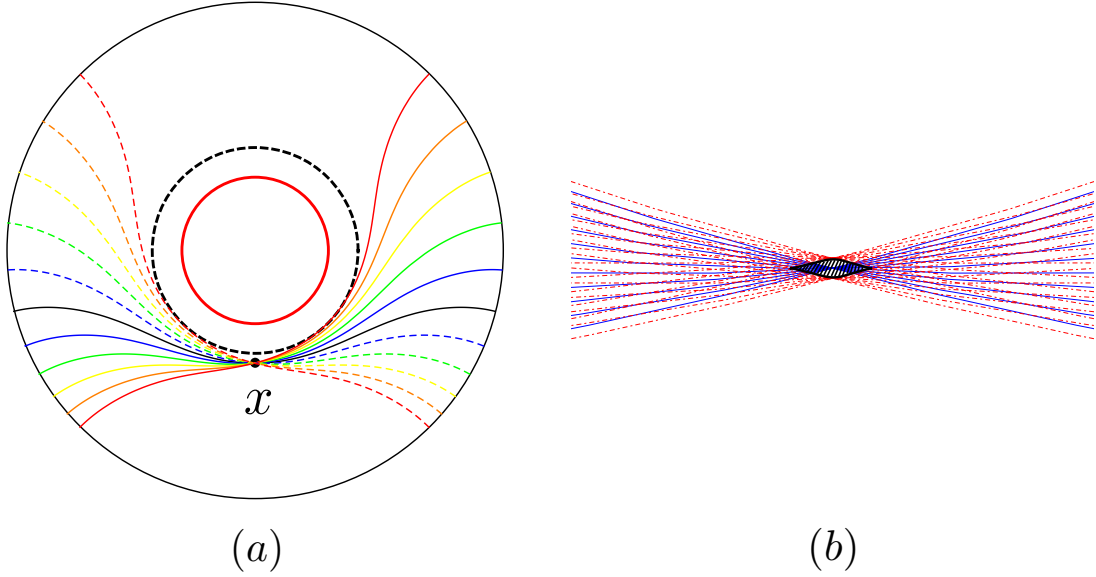


Figure 3: (a) The geodesics that cross the bulk point x outside the entanglement shadow (the dashed black circle) in the BTZ blackhole geometry with the metric $ds^2 = -(r^2 - b^2)dt^2 + (r^2 - b^2)^{-1}dr^2 + r^2d\phi^2$. The red circle is the horizon $r = b$. We take $b = 0.5$ in this calculation. We use coordinate $l = \frac{2}{\pi} \tan^{-1}(r)$ to map the infinite space $r \in [0, \infty]$ to a finite disk $l \in [0, 1]$. (b) A zoom-in picture of the intersection of expansions of geodesics crossing x . The overlap of the expanded geodesics gives the upper bound of causal future of x , which is the diamond shape region with corners, because the geodesics only cross x from a finite angle range.

boundary region A is a space-time region E_A which is the domain of dependence for any space-like surface bounding A and the extremal surface γ_A , as is illustrated in Fig.4 (a). Any bulk operator in E_A in the code subspace can be locally reconstructed on A . [8–11]

We start from a boundary spatial region A at boundary time $t = 0$, and a bulk point x on the corresponding extremal surface γ_A bounding A . (Again x should be understood as actually an infinitesimal distance to γ_A so that x is included in E_A .) An operator ϕ_x at x can be reconstructed in region A as $O_A[\phi_x]$. We would like to determine the butterfly velocity $v(O_A[\phi_x]; \mathcal{H}_c)$ of this operator in code subspace \mathcal{H}_c . (The code subspace is spanned by low energy excitations in the bulk that cause negligible back reaction.)

We first state our conclusion. As has been defined in Eq. (4), we denote the expansion of region A by a size $v\Delta t$ as $A_{v\Delta t}$. If operator O_A grows with butterfly velocity v , it will spread to a region $A_{v\Delta t}$ at time Δt , as is illustrated in Fig.4(b). Denote v^* as the minimal velocity such that the entanglement wedge $E_{A_{v\Delta t}}$ of $A_{v\Delta t}$ includes x . We claim that $v^* = v(O_A[\phi_x], \mathcal{H}_c)$ is the butterfly velocity of $O_A[\phi_x]$.

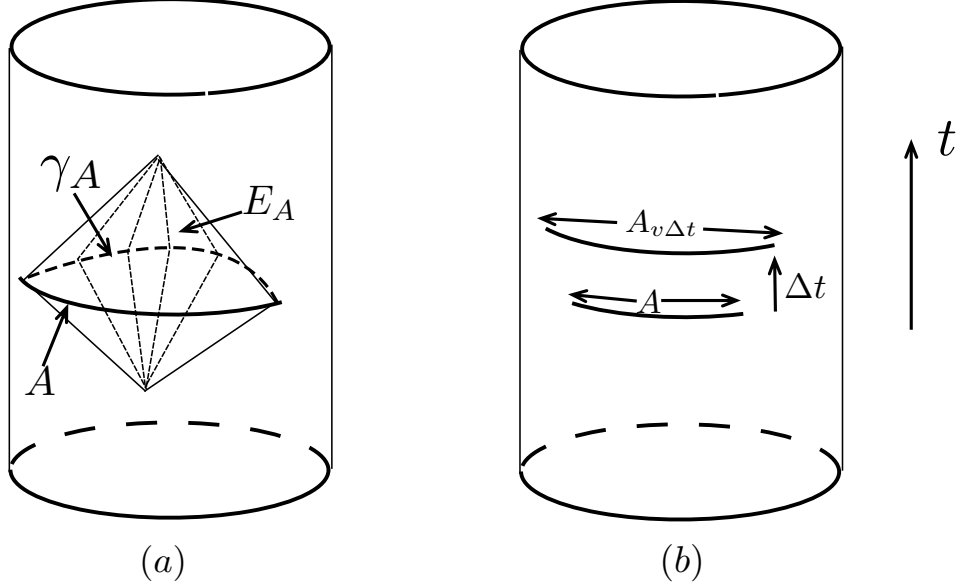


Figure 4: (a) Illustration of the entanglement wedge of a boundary region A . The vertical axis is the time direction and the boundary of the cylinder represents the boundary theory. The dashed curve γ_A is the extremal surface bounding the region A . The entanglement wedge E_A is the domain of dependence of the bulk region enclosed by $\gamma_A \cup A$. The thin straight lines are null geodesics. (b) The relation of region A and its expansion $A_{v\Delta t}$ by speed v .

To prove this conclusion, we need to prove two conditions. 1) Any operator on the complement of $A_{v^*\Delta t}$ (at time Δt) commutes with $O_A[\phi_x]$. This proves the butterfly velocity $v(O_A[\phi_x]) \leq v^*$. 2) For any velocity $v < v^*$, one can find operator on the complement of $A_{v\Delta t}$ that does not commute with ϕ_x . This proves $v(O_A[\phi_x]) = v^*$.

We start from the first condition. By definition of v^* , ϕ_x can be reconstructed on the boundary as an operator $O_{A_{v^*\Delta t}}[\phi_x]$ in region $A_{v^*\Delta t}$ at time Δt . For any boundary operator $O_B(\Delta t)$ supported in a region B at time Δt that does not intersect $A_{v^*\Delta t}$, we have

$$\langle \psi_i | [O_A[\phi_x], O_B(\Delta t)] | \psi_j \rangle = \langle \psi_i | [\phi_x, O_B(\Delta t)] | \psi_j \rangle = \langle \psi_i | [O_{A_{v^*\Delta t}}[\phi_x], O_B(\Delta t)] | \psi_j \rangle = 0 \quad (7)$$

for any pair of states $|\psi_i\rangle, |\psi_j\rangle \in \mathcal{H}_c$. Therefore the butterfly velocity $v(O_A[\phi_x], \mathcal{H}_c) \leq v^*$.

Now we prove the second condition. By definition of v^* , for any $v < v^*$ the entanglement wedge $E_{A_{v\Delta t}}$ will not include x . Denote the complement of $A_{v\Delta t}$ as C , as is shown in Fig. 5 (b). Since $x \notin E_{A_{v\Delta t}}$, the future of x has a nontrivial intersection of E_C . In other words, there exists a bulk point $y \in E_C$ that is time-like separated to x . For a generic operator ϕ_x , there exists operator ϕ_y which does not commute with ϕ_x . Denote

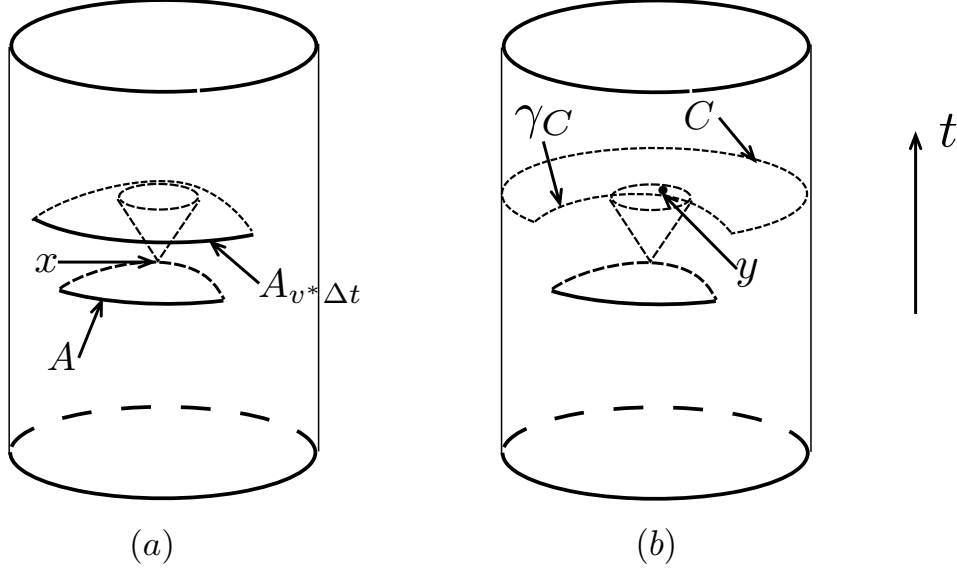


Figure 5: The setup that determines the butterfly velocity v^* . (a) For a region A at boundary time 0 and a point x on the extremal surface bounding A , v^* is chosen such that the extremal surface bounding the expanded region $A_{v^* \Delta t}$ at a later time Δt is tangential to the light cone of x . In other words, x is at the boundary of the entanglement wedge of $A_{v^* \Delta t}$. (b) An illustration why v^* defined in (a) is the butterfly velocity. If we expand region A by any velocity slower than v^* , the entanglement wedge of the complement region (C) will have a nontrivial intersection with the causal future of x . Therefore one can find operators in the intersection region which are reconstructed to C and does not commute with ϕ_x . This demonstrate that the boundary dual of ϕ_x really expand with speed v^* .

$O_C[\phi_y]$ as the reconstruction of ϕ_y on region C , we concluded that there exists some states $|\psi_i\rangle, |\psi_j\rangle \in \mathcal{H}_c$, such that

$$\langle \psi_i | [\phi_x, \phi_y] | \psi_j \rangle \neq 0 \Rightarrow \langle \psi_i | [O_A[\phi_x], O_C[\phi_y]] | \psi_j \rangle \neq 0 \quad (8)$$

This proves that the butterfly velocity must be larger than v for any $v < v^*$. Therefore we reach the conclusion that v^* is equal to the butterfly velocity $v(O_A[\phi_x], \mathcal{H}_c)$.

We would like to emphasize that this protocol of determining the butterfly velocity is covariant, so that it applies to a generic geometry without time translation symmetry. In the following sections, we will study various properties of butterfly velocity based on this protocol. Although the duality is only established for asymptotic AdS geometries, it is well-defined to study the consequence of our protocol in even more general geometries, assuming the local reconstruction and HRT formula generalizes. For example, in Sec.7 we will apply this protocol to the flat space with a finite boundary, which provide conditions

that the holographic dual theory of a flat space weakly coupled gravity have to satisfy, if such theory exists.

5 General properties of butterfly velocity

5.1 Monotonicity

In this section, we obtain some general properties of the butterfly velocity based on the assumption that the bulk dual geometry satisfies Einstein equation (EE) and the null energy condition (NEC). In short, we show that among bulk local operators ϕ_x on the same extremal surface γ_A , the butterfly velocity is a non-increasing function of the distance from x to the boundary. Intuitively, operators in the infrared always move with a velocity that is smaller or equal to those in the ultraviolet. Our result applies to disk shape regions on a boundary geometry with spatial rotation symmetries.

In the following we will explain our result and provide an intuitive explanation of the main idea of the proof. The rigorous proof will be given in Appendix. B. We consider a disk shape region A on the boundary. When the boundary has rotation symmetry that preserves the disk A , the corresponding extremal surface γ_A also has rotation symmetry. Points on γ_A can be parametrized by Ω_{d-2} , the $d - 2$ dimensional angular coordinates, and z which parameterizes the direction perpendicular to the boundary. The boundary theory locates at $z = 0$ (see Fig.6 (a)). Consider a bulk operator $\phi(z, \Omega_{d-2})$ which is locally reconstructed to region A as a boundary operator $O_A[\phi(z, \Omega_{d-1})]$. Because of the rotational symmetry, it is clear that the butterfly velocity $v(O_A[\phi(z, \Omega_{d-1})], \mathcal{H}_c)$ only depends on z , which we will denote as $v_A(z)$. Our result is that for any two points at $z_1 < z_2$, $v_A(z_1) \geq v_A(z_2)$, as is illustrated in Fig.6 (b).

This monotonicity property results from the property of null expansion in geometries satisfying EE and NEC, which has also played an essential role in proving the entanglement wedge is outside the causal wedge in asymptotic AdS geometries [24, 25]. (To clarify, our result is not restricted to asymptotic AdS.) With more details reserved to Appendix B, here we would like to provide some intuitive illustration to the proof for the simplest case of static geometries. We start by considering the butterfly velocity of the operator at the “tip” of γ_A (the point with $z = z_m$ maximal), which is determined by the minimal surface $\tilde{\gamma}$ in Fig. 7. $\tilde{\gamma}$ is defined at boundary time Δt and has a distance $c\Delta t$ to the tip point. In other words, as Δt increases from 0, the tip point of $\tilde{\gamma}$ grows with bulk speed of light. The butterfly velocity of the tip point v_m is determined by the growth velocity of the boundary

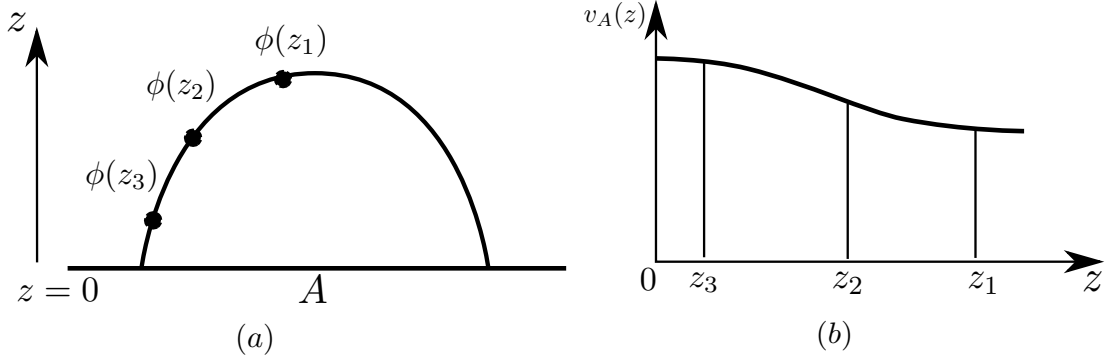


Figure 6: (a) Three bulk local operators $\phi(z_1), \phi(z_2), \phi(z_3)$ with decreasing distance to the boundary $z_1 > z_2 > z_3$, reconstructed to the same region A . (b) Schematic plot of butterfly velocity as a function of radial coordinate z which decreases monotonously when the operator moves deeper in the bulk.

position of $\tilde{\gamma}$. As is shown in Fig. 7, if $\tilde{\gamma}$ is anchored to a boundary disk that is bigger than A by x , the butterfly velocity of tip operators is $v_m = x/\Delta t$. Now we pick a different point at depth $z < z_m$. The distance of point z to the surface $\tilde{\gamma}$ is generically different from $c\Delta t$, which we denote as $u(z)\Delta t$. In other words, $u(z)$ is the speed of expansion of $\tilde{\gamma}$ at point z . To determine the butterfly velocity $v(z)$ of this point, one should consider another minimal surface that expands at z point with speed of light, and expands at the boundary with velocity $v(z)$. Note that the expansion speed at different locations of the surface are proportional to each other, we have

$$\frac{u(z)}{v_m} = \frac{c}{v(z)} \Rightarrow v(z) = \frac{c}{u(z)} v_m \quad (9)$$

Therefore the butterfly velocity of all points on γ_A can be determined by the single surface $\tilde{\gamma}$. To understand the general behavior of $u(z)$, we draw some surfaces $C(d)$ which has constant distance d to the surface γ_A (see Fig. 7). In space-time, such surfaces are obtained by null expansion of γ_A for time d/c . The key consequence of EE and NEC is that any extremal surface like $\tilde{\gamma}$ cannot be tangential to any $C(d)$ from outside [24–26]. In other words, either $\tilde{\gamma}$ coincide with $C(d)$ with $d = c\Delta t$ for all z , or $\tilde{\gamma}$ crosses $C(d)$ surfaces, in which case the distance $u(z)\Delta t$ has to decrease as z decreases. Consequently, $v(z) \propto 1/u(z)$ always increases or stays constant as z decreases towards the boundary. A more rigorous proof of this result is given in Appendix B.

One direct consequence of this result is that the butterfly velocity of all boundary operators are smaller or equal to the speed of light if the geometry is asymptotically

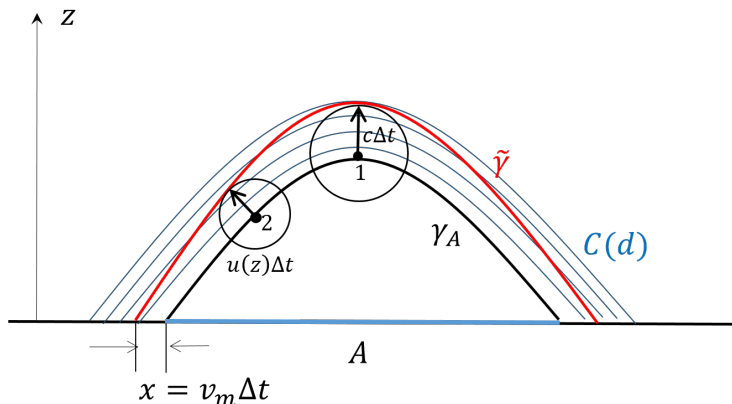


Figure 7: The setup in the proof of monotonicity of butterfly velocity (for the case of static geometries). The horizontal line at the bottom is the boundary at $z = 0$. The black thick curve represents extremal surface γ_A which bounds a boundary region A (blue thick line). The red curve stands for a minimal surface $\tilde{\gamma}$ that has a distance $c\Delta t$ to the tip point 1. At a different point 2 with depth z , $\tilde{\gamma}$ expands with a different speed $u(z)$ so that it is $u(z)\Delta t$ away from point 2. The blue thin curves $C(d)$ are expansion of γ_A by distance d for different d . The key of the proof is that $\tilde{\gamma}$ cannot be tangential to $C(d)$'s anywhere other than the tip point.

AdS. A straightforward calculation tells us that the butterfly velocity of all the operators are equal to the speed of the light for a pure AdS geometry (see Sec.6). Thus for an asymptotic AdS geometry, $\lim_{z \rightarrow 0} v_A(z) = c$. Consequently $v_A(z) \leq c$ for all z due to the monotonicity. This is consistent with our expectation that the boundary theory with the asymptotic AdS dual is relativistic. This is consistent with previously known results that there is no superluminal bulk signaling between boundary points [27–29]. In contrast, for geometries that are not asymptotically AdS, butterfly velocity can exceed speed of light even if the geometry satisfies EE and NEC. One example is the flat space, which we will study in Sec. 7.

5.2 When is the butterfly velocity equal to c ?

In the previous subsection, we have discussed that, for a boundary theory dual to an asymptotic AdS gravity that satisfies EE and NEC, the butterfly velocity of the boundary operators are less than or equal to the speed of the light. It is natural to ask in general when the upper bound is saturated. In this subsection we will prove that the entanglement wedge and causal wedge of a boundary region A coincide, then the butterfly velocity of all local operators on γ_A is equal to the speed of light $v(A; \mathcal{H}_c) = c$.

We will present the intuitive interpretation here and leave the rigorous proof in the Appendix.C. In order to prove that $v(A; \mathcal{H}_c) = c$ for all the generic operators when the causal wedge of A coincides with the entanglement wedge of A , we only need to show that the entanglement wedge of $A_{u\Delta t}$ does not contain any part of γ_A if $u < c$. γ_A is the entanglement surface of A which coincides with A 's causal surface. The entanglement wedge E_A is the domain of dependence of the region enclosed by $A \cup \gamma_A$ (Fig.8(a)). In Fig.8(b), the blue line is the extremal surface of the boundary region $A_{c\Delta t}$ and the red line is the extremal surface of the boundary region $A_{u\Delta t}$, where $u < c$. Because the causal wedge of A coincides with its entanglement wedge $C_A = E_A$, then obviously $C_{A_{u\Delta t}}$, the causal wedge of $A_{u\Delta t}$ (the red dashed line in Fig.8(b)), does not contain any part of γ_A if $u < c$. On the other hand, in the Appendix.C, we prove that, if $C_A = E_A$, then for the boundary regions that are sufficiently close to A , such as $A_{u\Delta t}$ and $A_{c\Delta t}$ with $\Delta t \rightarrow 0$, the difference between the entanglement wedges and the causal wedges are of $O(\Delta t^2)$. While the difference between $C_{A_{u\Delta t}}$ and $C_{A_{c\Delta t}}$ is of $O((c - u)\Delta t)$, thus as long as $u < c$, $E_{A_{u\Delta t}}$ does not contain any part of γ_A . Details are presented in Appendix.C.

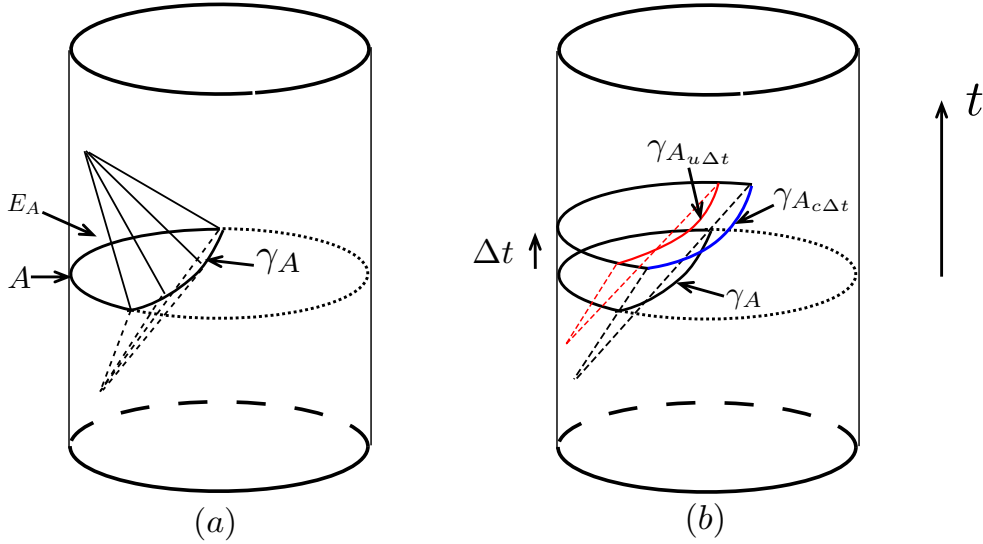


Figure 8: (a) Illustration of a region A with its entanglement wedge coincide with causal wedge. (b) For any velocity $u < c$, the entanglement surface of the expansion $A_{u\Delta t}$ (red solid curve) does not intersect with χ_A , so that the butterfly velocity $v^* > u$, which leads to the conclusion $v^* = c$.

6 Examples

6.1 Pure AdS and BTZ black hole

In this subsection, we follow our protocol in Sec.4, and calculate the butterfly velocities of operators in boundary theory whose bulk dual geometry is the $d + 1$ dimensional AdS space. A straightforward calculation shows us that the butterfly velocities are indeed the speed of light $c = 1$. This is consistent with our conclusion in Sec.5.2, since in pure AdS the causal wedges coincide with the entanglement wedges.

The metric of $d + 1$ dimensional AdS is $ds^2 = (-dt^2 + dz^2 + \sum_i dy_i^2)/z^2$. Since the space-time is translationally invariant in t and y_i , without loss of generality, we focus on the spherical boundary region A at $t = 0$ centered at $y_i = 0$. The radius of the boundary region is R , and the minimal surface γ that covers this boundary region is $\sum_i y_i^2 + z^2 = R^2$. For an arbitrary point x on the minimal surface, we can choose the coordinate so that $y_i(x) = 0$, $i = 2 \cdots d - 1$, thus $y_1(x)^2 + z(x)^2 = R^2$.

We then expand the radius of the boundary region a little bit to $R + \Delta R$ and the new minimal surface γ' is $\sum_i (y_i(x) + \Delta y_i)^2 + (z(x) + \Delta z)^2 = (R + \Delta R)^2$. γ' is located at time slice $t = \Delta t$. A straightforward calculation shows that the shortest distance between point x and γ' is

$$d(x, \gamma') = \frac{1}{z(x)^2} \min \left(\sum_i \Delta y_i^2 + \Delta z^2 - \Delta t^2 \right) = \frac{1}{z(x)^2} (-\Delta t^2 + \Delta R^2) \quad (10)$$

The butterfly velocity is determined by choosing a γ' that is lightlike separated from x , with $d(x, \gamma') = 0$. This requires $\Delta t = \Delta R$ and gives the butterfly velocity

$$v(O_A[\phi_x]; \mathcal{H}_c) = \frac{\Delta R}{\Delta t} = 1 \quad (11)$$

Since the $2 + 1$ BTZ blackhole is locally identical to pure AdS space, the butterfly velocity for the dual of bulk local operators outside the entanglement shadow of BTZ black hole is also equal to speed of light. This is consistent with our understandings that the butterfly velocities of operators in $1 + 1$ d CFT at the finite temperature is still c .

6.2 Higher dimensional AdS Schwarzschild black hole

In higher dimensions, butterfly velocities of operators in finite temperature systems are smaller than the speed of the light. The butterfly velocities of operators evolved after the scrambling time has been calculated in both the shock wave geometry approach [1, 6, 2]

and the near-horizon minimal surface approach [7]. Our result can be considered as a generalization of the latter.

In this subsection, we systematically study the butterfly velocities of operators in a finite temperature CFT in d dimensions, for which the bulk dual geometry is the $d + 1$ -dimensional AdS Schwarzschild blackhole.

The metric of AdS Schwarzschild blackhole is

$$ds^2 = -U(r)dt^2 + U(r)^{-1}dr^2 + r^2 d\Omega_{d-1}^2 \quad U(r) = 1 - \frac{\mu}{r^{d-2}} + \frac{r^2}{l^2} \quad (12)$$

with l the AdS radius. μ is related to the black hole mass by $M = \Omega_{d-1}\mu(d-1)/(16\pi G_N)$, where Ω_{d-1} is the area of a $d - 1$ -dimensional unit radius sphere. For simplicity, we fix $l = 1$. In this coordinate, $r \rightarrow \infty$ is the boundary. For $d > 2$, the extremal surfaces do not have a nice analytic form, thus we numerically implement our protocol and calculate the butterfly velocities of generic operators supported on spherical boundary regions.

For rotation symmetric boundary region, the minimal surface is also rotation symmetric. The intersection of the minimal surface at a fixed radial coordinate r is a spherical cap on the sphere S^{d-1} . We can choose a coordinate $d\Omega_{d-1}^2 = d\theta^2 + \sin^2\theta d\Omega_{d-2}^2$ for the fixed r sphere, with $\theta = 0$ at the center of the sphere. The minimal surface is parameterized by a function $r(\theta)$. Besides, the geometry of AdS Schwarzschild black hole is static, so that the extremal surfaces live on a constant t slice. The area of this co-dimension 2 surface is

$$Area = \Omega_{d-2}(r \sin \theta)^{d-2} \sqrt{U(r)^{-1} \left(\frac{dr}{d\theta} \right)^2 + r^2} \quad (13)$$

$r(\theta)$ is determined by minimizing the area.

We specify a boundary region A by the maximal depth that A 's extremal surface penetrates into the bulk, given by $r_A(\theta = 0) = r_0$, and $\frac{dr_A}{d\theta}|_{\theta=0} = 0$. Then we find the solution $r_A(\theta)$ with this boundary condition, and another solution $\tilde{r}_A(\theta)$ with a slightly different boundary condition $\tilde{r}_A(0) = r_0 + \delta$, $\frac{d\tilde{r}_A}{d\theta}|_{\theta=0} = 0$, with $\delta \ll r_0$. From these two solutions, we can decide numerically the butterfly velocities of the boundary reconstruction of the bulk operator $\phi(r_x)$, which is located at $r = r_x$, $\theta_x = r_A^{-1}(r_x)$.

$$\begin{aligned} v(O_A[\phi(r_x)]; \mathcal{H}_c) &= \frac{\Delta\theta}{\Delta t} \Big|_{r \rightarrow \infty} \\ \Delta\theta|_{r \rightarrow \infty} &= \tilde{r}_A^{-1}(\infty) - r_A^{-1}(\infty) \\ \Delta t|_{r \rightarrow \infty} &= \sqrt{\frac{\min_{\theta} [U(r_x)^{-1}(r_x - \tilde{r}_A(\theta))^2 + r_x^2(\theta_x - \theta)^2]}{U(r_x)}} \end{aligned} \quad (14)$$

We plot the butterfly velocities $v(O_A[\phi(r_x)]; \mathcal{H}_c)$ of the boundary reconstructions of the bulk operators $\phi(r_x)$ living on the background of $3+1$, $4+1$, $5+1$ AdS Schwarzschild black hole (Fig.9). The black horizontal lines are $\sqrt{\frac{d}{2(d-1)}}$, the butterfly velocity predicted by [1,6,2,7] of the operators evolved after the scrambling time. d is the spatial dimension of the bulk geometry. Each curve corresponds to the butterfly velocity of points on a minimal surface with fixed r_0 .

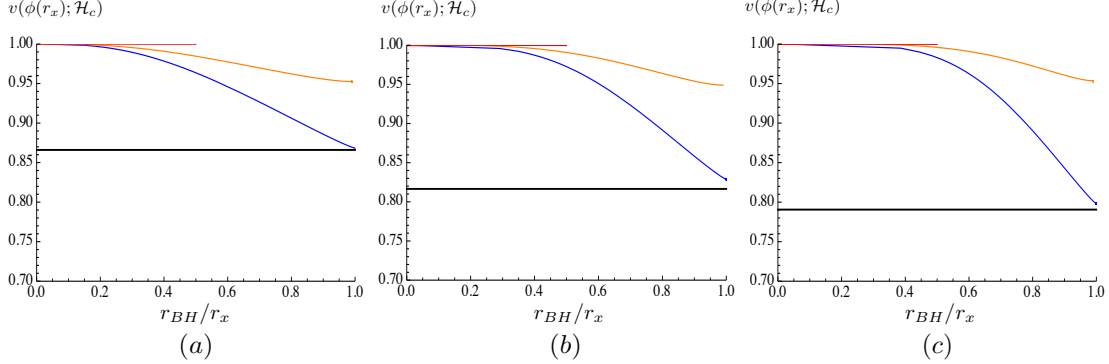


Figure 9: (a), (b), (c) are plots of the butterfly velocities $v(\phi(r_x); \mathcal{H}_c)$ of the boundary reconstructions of the bulk operators $\phi(r_x)$ in $3+1$, $4+1$, $5+1$ -dimensional AdS Schwarzschild black hole, respectively. The black lines is the reference value $\sqrt{d/2(d-1)}$, with d the bulk spatial dimension. Each curve corresponds to the butterfly velocity of operators on a minimal surface as a function of their radial coordinates. The red and orange curves correspond to minimal surfaces with tip at radial coordinate $r_0 = 2r_{BH}$, $(1 + 10^{-2})r_{BH}$, respectively. The blue lines in (a), (b), (c) correspond to $r_0 = (1 + 10^{-4})r_{BH}$, $(1 + 4 \times 10^{-5})r_{BH}$, $(1 + 8 \times 10^{-6})r_{BH}$, respectively. Here r_{BH} is the location of the horizon.

In Fig.9, we confirmed our conclusion in Sec. 5.1 that for spherical boundary regions, the butterfly velocities of the reconstructed operators decrease monotonically when its corresponding bulk operator moves to the IR. We also notice that the butterfly velocity approaches the universal IR value $\sqrt{\frac{d}{2(d-1)}}$ only when the bulk operators are extremely close to the horizon.

It is interesting to note that due to translation symmetry, the points on different curves in Fig.9 with the same r coordinate can be considered as different boundary local reconstructions of the same bulk operator (Fig.10). Although these different reconstruction operators all act identically in the code subspace, they act differently outside the code subspace, and have different butterfly velocities. Our numerical result indicates that the reconstructed operator in a bigger region (bounded by a minimal surface with smaller r_0) always has a smaller butterfly velocity. It is interesting to ask whether there is any monotonicity of butterfly velocity as a function of operator size. For general geometries

this is clearly not true, since we can consider a geometry which is vacuum in IR and has matter in UV which are falling in. For certain local operators in the bulk, we can find local reconstructions in a big region that is completely in the vacuum, while smaller reconstructions have to enter the region with matter, so that the butterfly velocity is maximal for the former. It is an interesting question whether the monotonicity in operator size is correct for a restricted class of geometries, such as static geometries with translation and rotation symmetry. It is still interesting if that is true. We leave this as an open question for future works.

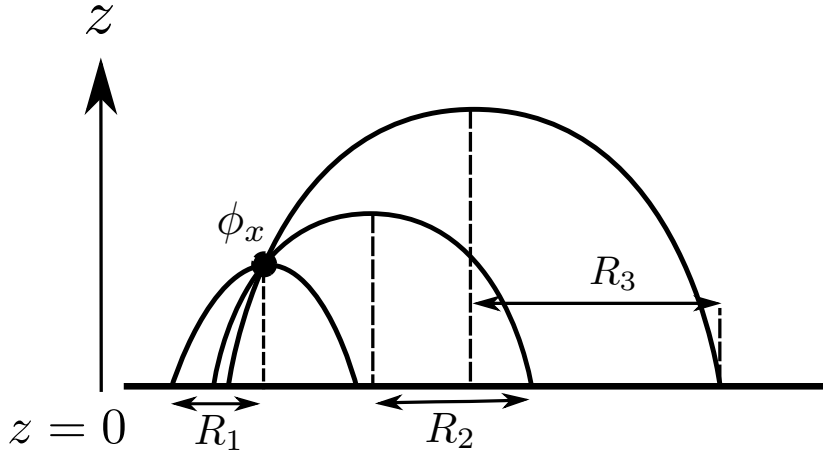


Figure 10: The same operator ϕ_x locally reconstructed to boundary regions R_1 , R_2 , R_3 with different size. Whether there is a monotonicity of the butterfly velocity vs size of the region is an open question.

7 Flat space

Since our general framework makes no assumptions on the geometry, it is natural to generalize our discussion to bulk geometries that are not asymptotic AdS. Although holographic duality has not been generalized to other geometries, the concepts such as HRT surface, entanglement wedge and causal wedge, etc., are well-defined for any Riemann geometry with a boundary.² Therefore we can ask the following question: If there is a boundary

²In asymptotic AdS geometry the boundary is conformal boundary, while in general geometry we may consider a boundary at a finite location. For a finite boundary the gravity is not decoupled from the

theory which is dual to a given bulk geometry, in the sense that local reconstruction properties apply to bulk low energy operators in the same way as the asymptotic AdS case, how will this boundary theory look like? The HRT formula for FRW geometries with a spherical boundary has been studied in Ref. [30, 31], which shows that the entanglement entropy of the boundary follows a volume law. In the following, we will study this problem for the flat space with a spherical boundary, from the point of view of butterfly velocities. Following our protocol in Sec. 4, we will find conditions on butterfly velocities that have to be satisfied for any possible dual of flat space gravity. In particular, we found that the butterfly velocity is not bounded from above, which indicates that the dual theory of flat space gravity, if exists, has to be nonlocal. This is consistent with the high entanglement entropy found in Ref. [30, 31].

We consider the $d + 1$ -dimensional flat space with the metric

$$ds^2 = -dt^2 + dr^2 + r^2 d\theta^2 + r^2 \sin^2 \theta d\Omega_{d-2}^2 \quad (15)$$

and a spherical boundary at $r = \Lambda$. The induced metric of the boundary is $ds^2 = -dt^2 + \Lambda^2 d\theta^2 + \Lambda^2 \sin^2 \theta d\Omega_{d-2}^2$.

We focus on the butterfly velocity of the reconstruction of bulk local operators on disk regions. A disk region centered at $\theta = 0$ point is defined by $r = \Lambda$, $\theta \in [0, \Theta]$. The disk region is a cap on the boundary sphere, and the minimal surface is a flat disk bounding the cap, as is illustrated in Fig. 11. The calculation of butterfly velocity is straightforward. Here we will list the main results and leave more detail of the explicit calculation in Appendix.D.

1. For operators ϕ_x at different location of the same minimal surface, their reconstruction $O_A[\phi_x]$ on the same boundary region all have the same butterfly velocity. This can be seen easily by applying the intuitive picture we discussed in Sec. 5.1. If we expand the boundary region by increasing Θ , the minimal surface stays flat so that it expands in the bulk with a constant velocity.
2. Due to the property 1 discussed above, the butterfly velocity $v_B[\phi_x] = v_B(\Theta)$ is only a function of the reconstructed operator size Θ . $v_B(\Theta)$ has the following form:

$$v(O_{A(\Theta)}; \mathcal{H}_c) = \frac{c}{\sin \Theta} \quad 0 \leq \Theta \leq \pi \quad (16)$$

boundary theory, but this does not affect our discussion here in the large N limit, since concepts like local reconstruction and entanglement wedge are all properties of the classical background geometry.

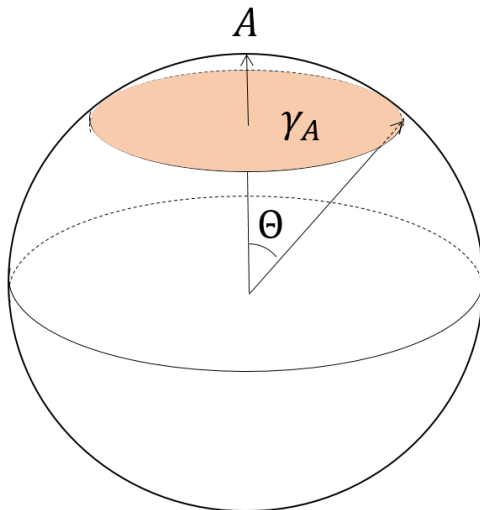


Figure 11: Illustration of the flat space with a spherical boundary. A boundary spherical cap region A parameterized by angle coordinate Θ is bounded by a flat minimal surface γ_A .

Therefore the butterfly velocity of boundary operators diverge in the small size limit $\Theta \rightarrow 0$. The bulk speed of light is actually the lower bound of v_B , which is reached by biggest operators that occupy half of the boundary.

Therefore we have shown that the dual of flat space gravity, if exists, must have a divergent Lieb-Robinson velocity, which requires the Hamiltonian to be nonlocal. Conversely, we can also apply the discussion in Sec. 3 to the flat space case. If we assume the boundary theory is a Lorentz invariant theory and is mapped to a bulk theory on flat space (say by a tensor network), we conclude that the bulk light cone has to have a strange shape. The speed of light in the direction perpendicular to the boundary for a bulk point x has to vanish as the point approaches the boundary. It is interesting to generalize this discussion to more generic geometries such as the FRW geometry studied in Ref. [30, 31].

8 Conclusion and discussion

In conclusion, in this paper we provide a general definition of butterfly velocity, which characterizes the propagation velocity of an operator measured in a given code-subspace. For large N theories with a gravity dual, we show that the quantum error correction properties in local reconstruction of bulk operators closely relates the bulk causal structure and the boundary butterfly velocities.

This relation is bidirectional. In the direction from the boundary to the bulk, we show that the Lieb-Robinson velocity of the boundary theory constrains the location of the bulk light cone, which guarantees that a local boundary theory is mapped to a bulk theory that appears local in the code subspace. In the direction from the bulk to the boundary, the bulk speed of light and extremal surfaces determine the butterfly velocity of boundary operators which are dual to bulk local operators. This correspondence has many consequences. For a spherical region in rotation invariant geometries, with the condition of EE and NEC we prove that the butterfly velocity of the dual of a bulk local operator decreases monotonously as the bulk operator moves from UV to IR. When the causal wedge of the boundary region A coincides with its entanglement wedge in an asymptotic AdS geometry (satisfying EE and NEC), the butterfly velocities of generic operators on A are exactly the speed of light. Explicit examples, including pure AdS and AdS Schwarzschild black holes in different dimensions, are studied, which confirm our new results and is consistent with the previous results [1, 2, 6, 7] in suitable limits. We have also applied our result beyond the standard AdS/CFT and obtain constraints on a possible dual theory of flat space gravity. We observe that in this case the boundary theory has to be nonlocal, with a diverging butterfly velocity for local operators.

There are many open questions that shall be studied in future works. In the black hole geometry we observe that different reconstruction of the same bulk operator has different butterfly velocities, and the reconstruction on a smaller region corresponds to a faster butterfly velocity. It is natural to search for more general constraints on the butterfly velocity as a function of the size of the boundary operator. Such relation may exist in general boundary theories, or may provide further conditions that a holographic theory has to satisfy.

Our discussion has focused on boundary operators that are local reconstruction of bulk local operators. If we generalize the discussion to more generic boundary operators that are dual to multi-point operators in the bulk, can we may obtain more general relation between the butterfly velocity of the boundary operator and the location of the dual bulk operator. For example, in the black hole geometry in $d + 1 > 3$, it is reasonable to believe there is only one boundary operator with the slowest butterfly velocity, which is dual to the local operator at the tip. If a given boundary operator has a butterfly velocity that is above the minimal value but smaller than speed of light, we know it cannot contain the faster operators living on the UV part of the minimal surface. In general, for a given boundary operator, its butterfly velocity may limit its dual operator to a subregion of the entanglement wedge.

The correspondence between boundary butterfly velocities and bulk causal structure may also provide a tool to determine bulk dual geometry for a boundary theory. In the context of holographic tensor networks, there is no a priori constraints on the bulk geometry. In principle, one can determine the bulk light cone if butterfly velocities of all boundary operators are known. It is a nontrivial requirement that the light cone is consistent with that of a Riemannian space-time geometry. This provides a possible way to constraint the choice of geometry for defining tensor network holographic mappings for a given boundary theory. For example one may define a holographic mapping with a flat space tensor network and apply it to a CFT ground state on the boundary. Our results suggest that the bulk low energy theory will not be Lorentz invariant, which suggests that the flat space is not the right choice for the tensor network representation of a CFT ground state.

Relation between the boundary theory and bulk causal structure has also been investigated in different approaches [32–34]. It is interesting to investigate the relation of these approaches with our results.

Acknowledgement. We acknowledge helpful discussions with Patrick Hayden, Isaac H. Kim, Aitor Lewkowycz, John Preskill, Stephen H Shenker and Michael Walter. This work is supported by the National Science Foundation through the grant No. DMR-1151786 (XLQ and ZY) and the David and Lucile Packard foundation (XLQ).

A Precise definition of butterfly velocity

The definition of butterfly velocity in Sec.2 involves the limit $\Delta t \rightarrow 0$. We will make it precise using the $\epsilon - \delta$ definition.

Precisely, the butterfly velocity $v(O_A; \mathcal{H}_c)$ can be defined given a boundary code subspace \mathcal{H}_c and a generic boundary operator O_A acting in region A . The definition is that for all $\epsilon > 0$, there exists $\delta > 0$, such that as long as $\Delta t < \delta$, the following two statements are satisfied.

1. If $D > (v(O_A; \mathcal{H}_c) + \epsilon) \Delta t$, then $\forall B \in \{R | d(R, A) = D\}$, and $\forall O_B$ supported in region B , $\forall |\psi_i\rangle, |\psi_j\rangle \in \mathcal{H}_c$,

$$\langle \psi_i | [O_A, O_B(\Delta t)] | \psi_j \rangle = 0 \quad (17)$$

2. If $D < (v(O_A; \mathcal{H}_c) - \epsilon) \Delta t$, then $\exists B \in \{R | d(R, A) = D\}$, and $\exists O_B$ supported in

region B , $\exists |\psi_i\rangle, |\psi_j\rangle \in \mathcal{H}_c$,

$$\langle \psi_i | [O_A, O_B(\Delta t)] | \psi_j \rangle \neq 0 \quad (18)$$

B Monotonicity of butterfly velocity of operators in the same region

In this section, we will prove that among all the bulk operators located at the extremal surfaces of a spherical boundary region, the deeper the bulk operator, the smaller the butterfly velocity of its reconstructed operator. Our proof applies to geometry of any dimensions with rotation symmetry and a rotation invariant boundary region, as long as it satisfies the Einstein equation (EE) and the null energy condition (NEC). In Fig.6 we illustrate the setup for 1+1 dimensional boundary theory with 2+1 dimensional bulk dual.

The tool we use in our proof is the null expansion in the general relativity, which has been used to prove that the entanglement wedge of a boundary region contains its causal wedge if the geometry satisfies EE and NEC [24,25]. We will introduce the important notions in this section. More details about the null expansion and Raychaudhuri equation can be found in textbooks about general relativity.

Let us start with boundary region A , bounded by the extremal surface γ_A . Then we shoot light-like geodesics perpendicular to γ_A pointing towards the boundary (Fig.12(a)). We define $U^\mu \equiv dx^\mu/d\tau$ to be the null vector along the null surface pointing towards the boundary. Since U^μ is null, we have the freedom to do affine transformation on τ . We scale τ so that when τ is a constant, it specifies a co-dimensional 2 surface that is perpendicular to U^μ and when $\tau = 0$, the co-dimensional 2 surface is exactly γ_A . Thus we have defined a one parameter family of co-dimensional 2 surfaces $\Gamma(\tau)$, and $h_{\mu\nu}(\tau)$ is the induced metric on $\Gamma(\tau)$. The null expansion θ is defined as

$$\theta[\Gamma(\tau)] = h^{\mu\nu}(\tau) \nabla_\mu U_\nu \quad (19)$$

The null expansion satisfies the Raychaudhuri equation

$$\frac{d\theta[\Gamma(\tau)]}{d\tau} = -\frac{1}{d-1}\theta^2 - \sigma_{\mu\nu}\sigma^{\mu\nu} - R_{\mu\nu}U^\mu U^\nu \quad (20)$$

where $\sigma_{\mu\nu}$ is the shear part of the extrinsic curvature. The important thing is that when the geometry satisfies EE,

$$R_{\mu\nu}U^\mu U^\nu = \left(8\pi G \left(T_{\mu\nu} - \frac{1}{d-1}Tg_{\mu\nu}\right) + \frac{2\Lambda g_{\mu\nu}}{d-1}\right)U^\mu U^\nu = 8\pi GT_{\mu\nu}U^\mu U^\nu \quad (21)$$

and NEC means $T_{\mu\nu}U^\mu U^\nu \geq 0$ if U^μ is null. Since $\sigma_{\mu\nu}\sigma^{\mu\nu}$ is also non-negative, we conclude that $\theta[\Gamma(\tau)]$, the null expansion, decreases monotonically along τ .

Now we will prove two lemmas first from which the monotonicity result can be deduced straightforwardly. As we have mentioned $\Gamma(0) = \gamma_A$, the extremal surface of the boundary region A . In our convention, $\tau > 0$ ($\tau < 0$) means the co-dimensional 2 surfaces are moving towards (away from) the boundary (Fig.12(a)).

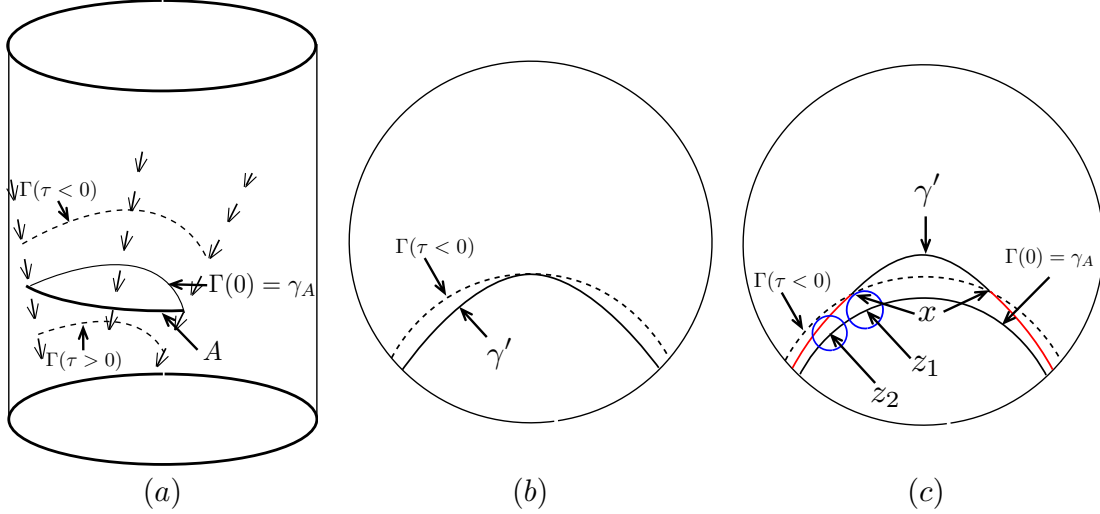


Figure 12: (a) Illustration of a null congruence of γ_A , the extremal surface bounding a boundary region A . The three straight lines with arrows are null geodesics emitted from and perpendicular to γ_A . $\Gamma(\tau > 0)$ and $\Gamma(\tau < 0)$ are two co-dimensional 2 surfaces belonging to the one parameter family $\Gamma(\tau)$ (see text). (b) Illustration of the setup in Lemma B.1. χ' is a geodesic surface that is tangential to $\Gamma(\tau < 0)$ in figure (a). (For simplicity, only spatial directions are drawn, but the two surfaces are not required to be in a certain constant time surface.) (c) Illustration of the setup in Lemma B.2. x is the point where γ' intersects with $\Gamma(\tau < 0)$. z_1 and z_2 are two bulk points on γ_A . The blue circles are the light cones of z_1 and z_2 . γ' is tangential to the light cone of z_1 and intersects with that of z_2 .

Lemma B.1. *If an extremal surface γ' is tangent to the surface $\Gamma(\tau < 0)$ at its tip (Fig.12(b)), it will not intersect with the null congruence $\Gamma(\tau)$ again.*

Proof. One useful result that we will refer to has been proven in [24, 25]. If two co-dimensional 2 surfaces N_1 and N_2 are tangent at x , and if the null expansions of the null congruence emitted from N_1 and N_2 satisfy $\theta[N_1] \geq \theta[N_2]$, then in any sufficiently small neighborhood of x , N_2 is contained by the space-time region separated by the null congruence of N_1 towards the direction where the null congruence is pointing. Because

$\Gamma(0)$ is the extremal surface of the boundary region A , the null expansion is $\theta[\Gamma(0)] = 0$. According to the Raychaudhuri equation, the null expansion decreases monotonically with respect to τ . Thus the null expansion of $\Gamma(\tau < 0)$ is $\theta[\Gamma(\tau < 0)] \geq 0$. Because γ' is the extremal surface, $\theta[\gamma'] = 0$. Since γ' is tangent to $\Gamma(\tau < 0)$ at its tip, and $\theta[\Gamma(\tau < 0)] \geq \theta[\gamma']$, we conclude that for a sufficiently small region near the tip, the space-time region that is separated by $\Gamma(\tau)$ and contains the boundary A includes γ' .

Now, we need to prove that γ' does not get out of $\Gamma(\tau < 0)$ when we are moving away from the tip. In other words, the situation shown in Fig.13(a) does not happen. Assume that Fig.13(a) does happen, then we shrink the size of the boundary region A , so that $\Gamma(\tau < 0)$ deforms continuously into $\tilde{\Gamma}$ and is tangent to γ' at one point. Since $\tilde{\Gamma}$ is tangent to and inside γ' , we have $\theta[\tilde{\Gamma}] < \theta[\gamma'] = 0$. This is a contradiction since $\tilde{\Gamma}$ is the causal future of the extremal surface of some boundary region smaller than A , so that $\theta[\tilde{\Gamma}] \geq 0$ according to the Raychaudhuri equation. Therefore we conclude that Fig.13(a) does not happen. \square

Lemma B.2. *For a geodesic surface γ' which intersects with $\Gamma(\tau < 0)$ at a point x , then the points on γ' that are closer to the boundary (red part in Fig.12(c)) than x will not intersect with $\Gamma(\tau)$.*

Proof. The proof of this lemma only requires to exclude the situation in Fig.13(b), which can be ruled out following the same reasoning as the proof of Lemma B.1. \square

These two lemmas leads to the monotonicity result. In Fig.12(c), z_1 and z_2 are two points on $\Gamma(0) = \gamma_A$. (It should be noted that γ_A and γ' are at different boundary time, although for the purpose of illustration we have only drawn the spatial directions.) By construction, γ' is the minimal surface that is tangent to the light cone of z_1 (the blue circle around z_1), thus the distance between γ' and γ_A on the boundary decides the butterfly velocity of z_1 . To decide the butterfly velocity of z_2 , we notice that γ' intersects with the lightcone of z_2 . Thus we must increase the size of the boundary region enclosed by γ' to find the minimal surface that is tangent to the light cone of z_2 . Thus the butterfly velocity of z_2 is bigger than that of z_1 .

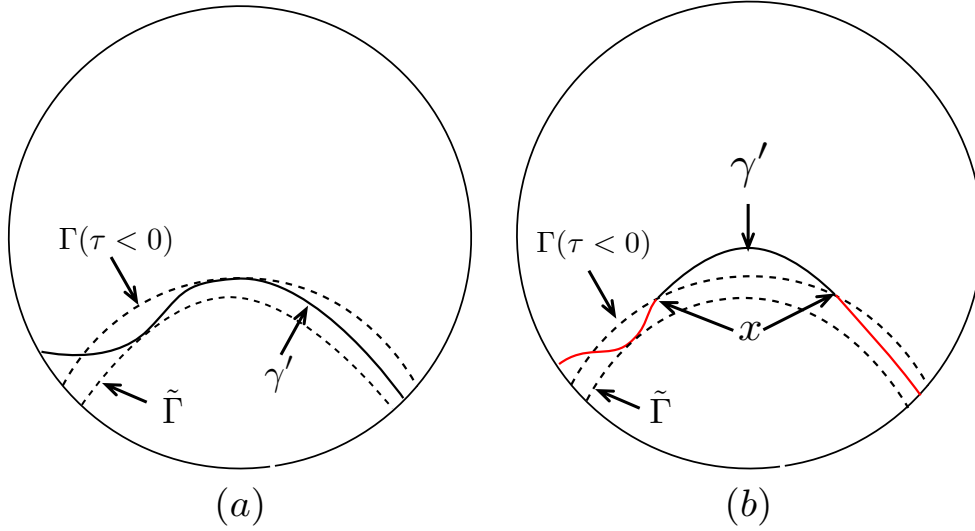


Figure 13: Two hypothetical situations that do not occur for geometries satisfying EE and NEC. $\Gamma(\tau < 0)$ is the causal future of γ_A , the extremal surface of the boundary region A (see. Fig. 12 (a)). (a) γ' is an extremal surface which is tangential to $\Gamma(\tau < 0)$. If γ' intersects with $\Gamma(\tau < 0)$ again, one can shrink the boundary region bounding γ' and find another extremal surface $\tilde{\Gamma}$ that is tangential to $\Gamma(\tau < 0)$ and is between $\Gamma(\tau < 0)$ and the boundary. (b) The same argument applies to a γ' that intersects with $\Gamma(\tau < 0)$ at point x .

C Proof of the saturation of butterfly velocity when the causal wedge coincides with the entanglement wedge

In this section, the assumptions we make on the bulk geometry are that 1) it is asymptotic AdS; 2) it satisfies the Einstein equation(EE), and null energy condition(NEC). We prove that when the causal wedge and the entanglement wedge of a boundary region coincide, the butterfly velocity of generic operators supported on this boundary region is c .

In Fig.14, the green curve in the middle is χ_A , the causal surface of the boundary region A , which coincides with γ_A , the entanglement surface of the boundary region A . The other two green curves are the causal surfaces of $A_{c\Delta t}$ and $A_{c(-\Delta t)}$, the expansion of boundary region A by speed of light c to time Δt . The two red curves are the causal surfaces of $A_{u\Delta t}$ and $A_{u(-\Delta t)}$ with a velocity $u < c$, and the two blue curves are the entanglement surfaces of $A_{u\Delta t}$ and $A_{u(-\Delta t)}$. It has been proven that the entanglement surfaces lie outside or coincide with the causal surfaces [24,25] for the asymptotic AdS geometry that satisfies EE and NEC. Thus the entanglement surfaces of the series of the boundary regions $A_{u,\tau}$

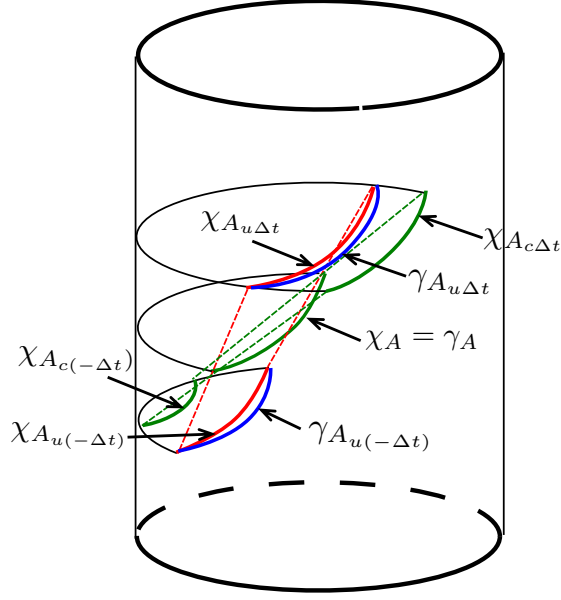


Figure 14: The setup in Sec. C. The green curves are the causal surfaces of three boundary regions, A , its expansion $A_{c\Delta t}$ and contraction $A_{c(-\Delta t)}$, respectively. The causal surface χ_A of the boundary region A coincides with its entanglement surface γ_A . The two red curves are the causal surfaces of $A_{u\Delta t}$, $A_{u(-\Delta t)}$ for $u < c$, respectively. The two blue curves are the entanglement surfaces of $A_{u\Delta t}$ and $A_{u(-\Delta t)}$, respectively.

$\tau \in [-\Delta t, \Delta t]/\{0\}$, will not penetrate into their causal surfaces and at least at $\tau = 0$, the two surfaces coincide. Now, we pick an arbitrary curve $x(\tau)$, $\tau \in [-\Delta t, \Delta t]$ such that $x(\tau)$ lives on the causal surface $\chi_{A_{u\cdot\tau}}$. Correspondingly, $y(\tau)$ is the point on the entanglement surface $\gamma_{A_{u\cdot\tau}}$ that is closest to $x(\tau)$. Because the distance $d(x(\tau), y(\tau))$ is 0 at $\tau = 0$ and $y(\tau)$ does not cross $x(\tau)$ when $\tau \in [-\Delta t, \Delta t]$, the curves are tangential to each other at $\tau = 0$, and we have

$$d(x(\tau), y(\tau)) = O(\tau^2), \quad \tau \in [-\Delta t, \Delta t] \quad (22)$$

On the other hand, because $u < c$, for $\tau \in [-\Delta t, \Delta t]$, $\chi_{u\cdot\tau}$ and $\chi_{c\cdot\tau}$ cross each other at $\tau = 0$. Thus if we pick an arbitrary curve $x(\tau)$, $\tau \in [-\Delta t, \Delta t]$ such that $x(\tau)$ lives on the causal surface $\chi_{A_{u\cdot\tau}}$, and $y(\tau)$ being the closest point to $x(\tau)$ living on the causal surface $\chi_{A_{c\cdot\tau}}$, the distance between $x(\tau)$ and $y(\tau)$ is

$$d(x(\tau), y(\tau)) = O((c - u)\tau), \quad \tau \in [-\Delta t, \Delta t] \quad (23)$$

Finally, we put these ingredients together. $\chi_A = \gamma_A$ means if $u < c$, the causal wedge $C_{A_{u\Delta t}}$ whose causal surface is $\chi_{A_{u\Delta t}}$ contains no part of γ_A , because the distance between any point on $\chi_{A_{u\Delta t}}$ and $\chi_{A_{c\Delta t}}$ is of order $O((c - u)\Delta t)$, while the distance between any

point on $\chi_{A_{u\Delta t}}$ and $\gamma_{A_{u\Delta t}}$ is of $O(\Delta t^2)$. Therefore we conclude that the butterfly velocity v of a local operator at γ_A must satisfy $v > u$ for any $u < c$. In other words, we must have $v = c$. In summary we conclude that the butterfly velocity of generic operators, supported on the boundary region of which the causal wedge coincide with the entanglement wedge is c .

D Flat space holography

We start from the $d + 1$ dimensional flat space metric. $ds^2 = -dt^2 + dr^2 + r^2 d\theta^2 + r^2 \sin^2 \theta d\Omega_{d-2}^2$. Because it is symmetric in time translation, we only need to focus on a single time slice to study the extremal surfaces. Besides, we will focus on the butterfly velocity of the boundary operators living on spherical regions, so that the boundary region is fully characterized by the size of the spherical cap, determined by the parameter Θ .

We set the boundary to be at $r = \Lambda$. Thus the induced boundary metric is $ds^2 = -dt^2 + \Lambda^2 d\theta^2 + \Lambda^2 \sin^2 \theta d\Omega_{d-2}^2$. At time t , the extremal surface that covers the boundary region $A = \{y | r = \Lambda, \theta \in [0, \Theta]\}$ is

$$r_\Theta(\theta) = \frac{\Lambda \cos \Theta}{\cos \theta}, \theta \in [0, \Theta] \quad (24)$$

Without loss of generality, we look at the bulk operator ϕ_x located on the extremal surface at point x , where $\theta = \theta_x$, $r = r_\Theta(\theta_x) = \frac{\Lambda \cos \Theta}{\cos \theta_x}$, $\vec{\Omega}_{d-2} = \vec{0}$. Now we find the extremal surface of the boundary region $[0, \Theta + \Delta\Theta]$ at time $t + \Delta t$

$$r_{\Theta+\Delta\Theta}(\theta) = \frac{\Lambda \cos(\Theta + \Delta\Theta)}{\cos \theta}, \theta \in [0, \Theta + \Delta\Theta] \quad (25)$$

The minimum of the proper distance between the bulk point x and the extremal surface $r_{\Theta+\Delta\Theta}(\theta)$ is

$$d(x, r_{\Theta+\Delta\Theta}(\theta)) = -c^2 \Delta t^2 + (\Lambda \sin \Theta \Delta\Theta)^2 \quad (26)$$

which is independent of θ_x , the angular position of x .

Thus in order for the entanglement wedge of the boundary region $[0, \Theta + \Delta\Theta]$ to include the point x , one needs to require

$$c\Delta t = \Lambda \sin \Theta \Delta\Theta \quad (27)$$

so that the butterfly velocity of the boundary reconstruction of ϕ_x is

$$v(O_A[\phi_x]; \mathcal{H}_c) = \frac{\Lambda \Delta\Theta}{\Delta t} = \frac{c}{\sin \Theta} \quad (28)$$

References

- [1] Stephen H Shenker and Douglas Stanford. Black holes and the butterfly effect. *arXiv preprint arXiv:1306.0622*, 2013.
- [2] Daniel A Roberts, Douglas Stanford, and Leonard Susskind. Localized shocks. *arXiv preprint arXiv:1409.8180*, 2014.
- [3] Juan Maldacena. The large-n limit of superconformal field theories and supergravity. *International journal of theoretical physics*, 38(4):1113–1133, 1999.
- [4] Edward Witten. Anti-de sitter space and holography. *Advances in Theoretical and Mathematical Physics*, 2:253–291, 1998.
- [5] Steven S Gubser, Igor R Klebanov, and Alexander M Polyakov. Gauge theory correlators from non-critical string theory. *Physics Letters B*, 428(1):105–114, 1998.
- [6] Daniel A Roberts and Brian Swingle. Lieb-robinson bound and the butterfly effect in quantum field theories. *Physical Review Letters*, 117(9):091602, 2016.
- [7] Márk Mezei and Douglas Stanford. On entanglement spreading in chaotic systems. *arXiv preprint arXiv:1608.05101*, 2016.
- [8] Ahmed Almheiri, Xi Dong, and Daniel Harlow. Bulk locality and quantum error correction in ads/cft. *arXiv preprint arXiv:1411.7041*, 2014.
- [9] Xi Dong, Daniel Harlow, and Aron C Wall. Reconstruction of bulk operators within the entanglement wedge in gauge-gravity duality. *Physical Review Letters*, 117(2):021601, 2016.
- [10] Daniel Harlow. The ryu-takayanagi formula from quantum error correction. *arXiv preprint arXiv:1607.03901*, 2016.
- [11] Xi Dong, Daniel Harlow, and Aron C Wall. Bulk reconstruction in the entanglement wedge in ads/cft. *arXiv preprint arXiv:1601.05416*, 2016.
- [12] Fernando Pastawski, Beni Yoshida, Daniel Harlow, and John Preskill. Holographic quantum error-correcting codes: Toy models for the bulk/boundary correspondence. *arXiv preprint arXiv:1503.06237*, 2015.

- [13] Zhao Yang, Patrick Hayden, and Xiao-Liang Qi. Bidirectional holographic codes and sub-ads locality. *Journal of High Energy Physics*, 2016(1):1–24, 2016.
- [14] Patrick Hayden, Sepehr Nezami, Xiao-Liang Qi, Nathaniel Thomas, Michael Walter, and Zhao Yang. Holographic duality from random tensor networks. *arXiv preprint arXiv:1601.01694*, 2016.
- [15] Xiao-Liang Qi, Zhao Yang, and Yi-Zhuang You. Holographic coherent states from random tensor networks. *arXiv preprint arXiv:1703.06533*, 2017.
- [16] William Donnelly, Ben Michel, Donald Marolf, and Jason Wien. Living on the edge: A toy model for holographic reconstruction of algebras with centers. *arXiv preprint arXiv:1611.05841*, 2016.
- [17] Maximo Banados, Claudio Teitelboim, and Jorge Zanelli. Black hole in three-dimensional spacetime. *Physical Review Letters*, 69(13):1849, 1992.
- [18] Elliott H Lieb and Derek W Robinson. The finite group velocity of quantum spin systems. In *Statistical Mechanics*, pages 425–431. Springer, 1972.
- [19] Bruno Nachtergaele, Yoshiko Ogata, and Robert Sims. Propagation of correlations in quantum lattice systems. *Journal of statistical physics*, 124(1):1–13, 2006.
- [20] MB Hastings. Locality in quantum systems. *arXiv preprint arXiv:1008.5137*, 2010.
- [21] Vijay Balasubramanian, Borun D Chowdhury, Bartłomiej Czech, and Jan de Boer. Entwinement and the emergence of spacetime. *arXiv preprint arXiv:1406.5859*, 2014.
- [22] Netta Engelhardt and Aron C Wall. Extremal surface barriers. *Journal of High Energy Physics (Online)*, 2014(03):68, 2014.
- [23] Veronika E Hubeny, Mukund Rangamani, and Tadashi Takayanagi. A covariant holographic entanglement entropy proposal. *Journal of High Energy Physics*, 2007(07):062, 2007.
- [24] Aron C Wall. Maximin surfaces, and the strong subadditivity of the covariant holographic entanglement entropy. *arXiv preprint arXiv:1211.3494*, 2012.
- [25] Veronika E Hubeny, Mukund Rangamani, and Erik Tonni. Global properties of causal wedges in asymptotically ads spacetimes. *arXiv preprint arXiv:1306.4324*, 2013.

- [26] Matthew Headrick, Veronika E Hubeny, Albion Lawrence, and Mukund Rangamani. Causality & holographic entanglement entropy. *arXiv preprint arXiv:1408.6300*, 2014.
- [27] Sijie Gao and Robert M Wald. Theorems on gravitational time delay and related issues. *Classical and Quantum Gravity*, 17(24):4999, 2000.
- [28] Netta Engelhardt and Sebastian Fischetti. The gravity dual of boundary causality. *arXiv preprint arXiv:1604.03944*, 2016.
- [29] Eric Woolgar. The positivity of energy for asymptotically anti-de sitter spacetimes. *Classical and Quantum Gravity*, 11(7):1881, 1994.
- [30] Yasunori Nomura, Nico Salzetta, Fabio Sanches, and Sean J Weinberg. Spacetime equals entanglement. *arXiv preprint arXiv:1607.02508*, 2016.
- [31] Yasunori Nomura, Nico Salzetta, Fabio Sanches, and Sean J Weinberg. Toward a holographic theory for general spacetimes. *arXiv preprint arXiv:1611.02702*, 2016.
- [32] Netta Engelhardt and Gary T Horowitz. Towards a reconstruction of general bulk metrics. *Classical and Quantum Gravity*, 34(1):015004, 2016.
- [33] Netta Engelhardt and Gary T Horowitz. Recovering the spacetime metric from a holographic dual. *arXiv preprint arXiv:1612.00391*, 2016.
- [34] Isaac H Kim and Michael J Kastoryano. Entanglement renormalization, quantum error correction, and bulk causality. *arXiv preprint arXiv:1701.00050*, 2016.